EPJ Web of Conferences **288**, 02002 (2023) https://doi.org/10.1051/epjconf/202328802002
ANIMMA 2023

R&D status for an innovative crystal calorimeter for the future Muon Collider

C. Cantone[1], S. Ceravolo[1], F. Colao[2], E. Di Meco[1,3,*], E. Diociaiuti[1], P. Gianotti[1], A. Liedl[1], D. Lucchesi[4], D. Paesani[1,3], N. Pastrone[5], G. Pezzullo[6], A. Saputi[7], I. Sarra[1], L. Sestini[4], D. Tagnani[8]

[1] INFN, Laboratori Nazionali di Frascati, Via Enrico Fermi 54, 00054 Frascati, Italy
[2] Enea Frascati, Via Enrico Fermi 45, 00044 Frascati, Italy
[3] Dipartimento di Fisica, Università degli Studi di Roma Tor Vergata, 00133 Roma, Italy
[4] INFN, Sezione di Padova, Via Francesco Marzolo 8, 35131 Padova, Italy
[5] INFN, Sezione di Torino, Via Pietro Giuria 1, 10125 Torino, Italy
[6] Yale University, New Heaven (CT), USA
[7] INFN, Sezione di Ferrara, Via Saragat 1I, 44122 Ferrara, Italy
[8] INFN, Sezione di Roma Tre, Via della Vasca Navale 84, 00146 Roma, Italy
(*) elisa.dimeco@lnf.infn.it

Abstract: **The measurement of physics processes at new energy frontier experiments requires excellent spatial, time, and energy resolutions to resolve the structure of collimated high-energy jets. Calorimeters, as other detectors, must face this increasing performance demand. In a future TeV-scale Muon Collider, the beam-induced background (BIB) represents the main challenge in the design of the detectors and of the event reconstruction algorithms and can pose serious limitations to the physics performance. However, it is possible to reduce the BIB impact on the Muon Collider calorimeter by exploiting some of its characteristics and by ensuring high granularity, excellent timing, longitudinal segmentation and good energy resolution. The proposed R&D is an innovative semi-homogeneous electromagnetic calorimeter based on stackable modules of lead fluoride crystals (PbF_2) readout by surface-mount UV-extended Silicon Photomultipliers (SiPMs): the Crilin calorimeter (CRystal calorImeter with Longitudinal INformation). The calorimeter should operate in a very harsh radiation environment, withstanding yearly a neutron flux of 10^{14} n_{1MeV} /cm^2 and a dose of 100 krad.**

In this paper, the radiation tolerance measured in several irradiation campaigns and the timing performances evaluated during a test beam at CERN-H2 with 120-GeV electron are discussed. A description of the latest prototype Proto-1, that will be shortly tested, is also provided.

Keywords — **Electromagnetic calorimeters, PbF_2, SiPM, Crystals, High Granularity.**

I. Introduction

NEW High Energy Physics research requires innovative accelerating machines to unlock the multi-TeV range. An interesting option is represented by a Muon Collider facility [1] which, with respect to hadronic machines, would be characterized by an exact knowledge of the initial state (free from parton density functions), by a limited QCD background and, with respect to an electron machine, would reach higher energies because of its very reduced bremsstrahlung losses. Nevertheless, many aspects have hindered the realization of such project: from the point of view of detectors construction one of the main challenges is represented by the Beam Induced Background (BIB). This BIB consists of a pervasive flux of secondary and tertiary particles coming from the interaction of the muons decay products with the machine elements creating a very harsh radiation environment. This means that the whole machine detector interface must be optimized in order to reduce as much as possible this huge contribution.

Concerning the electromagnetic calorimeter barrel the baseline solution consists of 64 million 5×5 mm^2 silicon sensors sampled with 40 layers of Tungsten for a total of 64 million readout channels [2], thus representing a significant technological issue as well as expensive. Indeed, other options are still under investigation. The presented R&D, the Crilin calorimeter [3], is one of the leading alternative choices for this purpose. It consists of a semi-homogeneous electromagnetic calorimeter made of Lead Fluoride Crystals (PbF_2) matrices where each crystal is readout by 2 series of 2 UV-extended surface mount SiPMs. Crilin was indeed optimized in the ambit of the Muon Collider experiment as a candidate design for an electromagnetic barrel calorimeter, because of its fine granularity, excellent timing resolution, good pileup capability and high resistance to radiation.

II. The Crilin calorimeter

The Crilin calorimeter Crilin has a modular architecture based on stackable and interchangeable sub-modules made of matrices of 10 × 10 × 40 mm^3 Lead Fluoride (PbF_2) crystals each readout by two series of two UV-extended 10 μm pixel-size Hamamatsu SiPMs with a surface of 3×3 mm^2 providing

© The Authors, published by EDP Sciences. This is an open access article distributed under the terms of the Creative Commons Attribution License 4.0 (https://creativecommons.org/licenses/by/4.0/).

a 36% coverage of the crystal area. The main features achievable with this choice are the following:

- High response speed since the Cherenkov response of PbF_2 is instantaneous with respect to the particle passage.
- Narrow signals therefore an excellent ability to resolve temporally close events at high rate leading to a good pileup capability.
- Good light collection that enables a good energy resolution throughout the whole dynamic range.
- Good resistance to radiation needed to withstand the Muon Collider harsh environment.
- Longitudinal segmentation that is crucial to distinguish signal showers from BIB.
- Fine granularity scalable with SiPMs pixel dimensions.

By adapting crystals transversal and longitudinal dimensions to maximize the signal/background ratio and choosing the proper SiPMs the goal is to achieve similar or better performance than the Si-W ECAL baseline solution. Indeed, the simulation framework of the International Muon Collider Collaboration has been employed to compare the performances of the two barrels. With this purpose the W-Si ECAL barrel used in this simulation framework has been substituted with Crilin. The full simulation of b-jets has been used for this purpose, and the beam-induced background was simulated as well. The jet reconstruction efficiency and jet p_T resolutions are presented in Figure 1. It can be noticed that the performances are similar in the two cases but, at the same time, the money cost of Crilin is a factor 10 less.

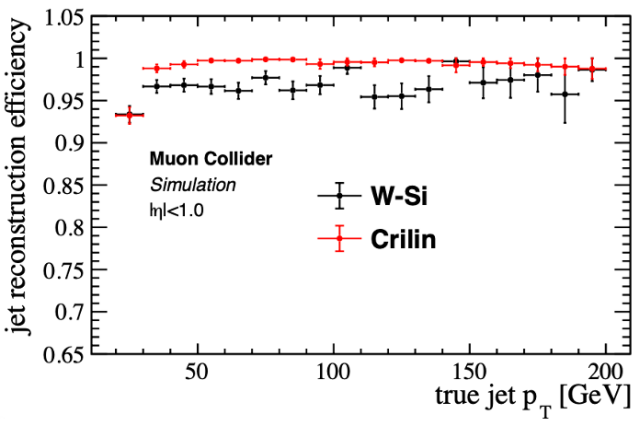

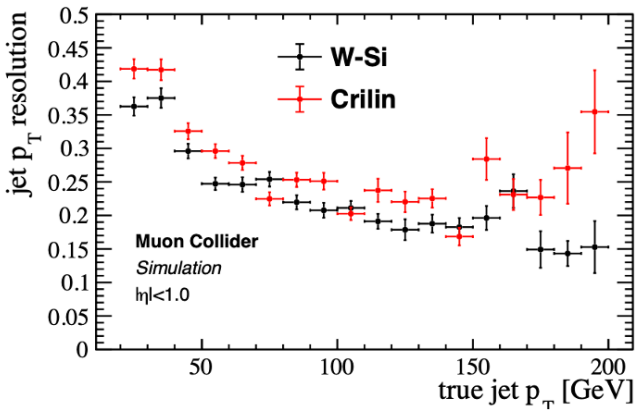

Fig. 1. Top-panel: jet reconstruction efficiency as a function of the jet p_T, obtained by using the Crilin ECAL barrel and the W-Si ECAL barrel. Bottom-panel: jet p_T resolution as a function of the jet p_T, obtained by using the Crilin ECAL barrel and the W-Si ECAL barrel.

A. Radiation hardness

Because of the Beam Induced Background a very harsh environment is expected for the Muon Collider. That is why a FLUKA [4] simulation at $\sqrt{s}$=1.5 TeV has been performed, thus resulting in the Total Ionizing Dose (TID) and neutron fluence levels showed in Figure 2.

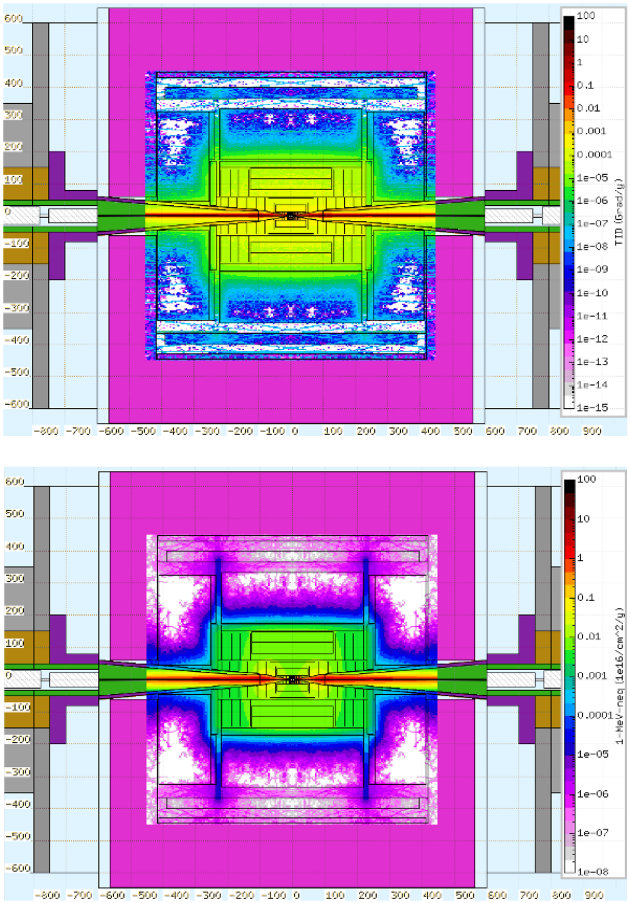

Fig. 2. TID (top) and 1-MeV-neq fluence (bottom) in the detector region for a Muon Collider operating at $\sqrt{s}$ = 1.5 TeV.

Regarding the ECAL barrel region the expected neutron fluence and dose are respectively 10^{14} $n_{1MeV}/(cm^2$ year) and 10^{-4} Grad/year.
Once the radiation levels were known it was necessary to check the radiation hardness of the single components of the calorimeter and to examinate different choices. Starting from crystals, as previously anticipated, the baseline choice for Crilin is represented by PbF_2. At the same time also $PbWO_4$-UF [5] appears to be a valid candidate, indeed this material embeds high density, good light yield, high radiation resistance and fast response speed since it combines both the prompt Cherenkov and a fast scintillation component, yielding a dominant emission with a decay time less then 700 ps.
In order to check the resistance to radiation of both crystals a TID irradiation campaign, after a preliminary one in 2021 [6], has been recently carried out at ENEA-Calliope facility with ^{60}Co. The resulting transmittance spectra after irradiation can be found in Figure 3 for both crystals. After a TID > 35 Mrad no significant decrease in transmittance observed for PbF_2, this happens also for $PbWO_4$-UF up to 100 Mrad.

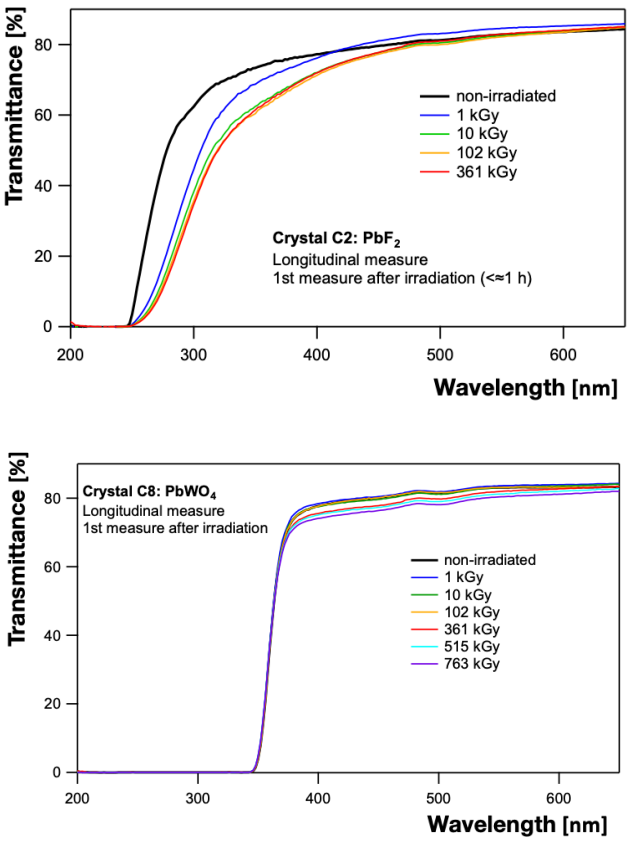

Fig. 3. Transmission spectra obtained in the different irradiation steps for the PbF_2 (top) and $PbWO_4$-UF (bottom) crystal samples.

A second irradiation campaign has been performed to check the radiation hardness of the SiPMs at the Frascati Neutron Generator (FNG-ENEA) facility with 14 MeV neutrons with a fluence up to 10^{14} n/cm^2. Neutron irradiation represents indeed one the main concerns when using these sensors since it leads to a significant increase of dark current. The sample under test were two: one series of 15 μm pixel-size and another one of 10 μm pixel-size Hamamatsu SiPMs. By measuring the amount of dark current after the irradiation at three different temperatures (the results are summarized in Table 1 and 2) it was clear that the right choice of SiPMs pixel-size in order to cope with the Muon Collider radiation environment was represented by the 10 μm once, since they have a more manageable dark rate contribution.

TABLE I
BREAKDOWN VOLTAGES AND DARK CURRENTS FOR 15 μM SIPMS

T [°C]	V_{br} [V]	$I(V_{br}+4V)$ [mA]	$I(V_{br}+6V)$ [mA]	$I(V_{br}+8V)$ [mA]
-10 ± 1	75.29 ± 0.01	12.56 ± 0.01	30.45 ± 0.01	46.76 ± 0.01
-5 ± 1	75.81 ± 0.01	14.89 ± 0.01	32.12 ± 0.01	46.77 ± 0.01
0 ± 1	76.27 ± 0.01	17.38 ± 0.01	33.93 ± 0.01	47.47 ± 0.01

TABLE 2
BREAKDOWN VOLTAGES AND DARK CURRENTS FOR 10 μM SIPMS

T [°C]	V_{br} [V]	$I(V_{br}+4V)$ [mA]	$I(V_{br}+6V)$ [mA]	$I(V_{br}+8V)$ [mA]
-10 ± 1	76.76 ± 0.01	1.84 ± 0.01	6.82 ± 0.01	29.91 ± 0.01
-5 ± 1	77.23 ± 0.01	2.53 ± 0.01	9.66 ± 0.01	37.51 ± 0.01
0 ± 1	77.49 ± 0.01	2.99 ± 0.01	11.59 ± 0.01	38.48 ± 0.01

B. Timing performances on a single crystal prototype

During 2022 a preliminary evaluation of the timing performances of Crilin has been carried out by means of a Beam Test at CERN-SPS beamline with 120-GeV electrons. The device under test consisted in a single layer prototype, Proto-0, with only one crystal readout by 2 series of 10 μm pixel-size Hamamatsu SiPMs connected to a custom Front End Electronics (discussed in Sec. III). The goals of this test were [7]: *i*) validate CRILIN new readout electronics and readout scheme *ii*) study systematics of light collection in small crystals with high refractive index *iii*) measure the time resolution achievable with different crystal choices, indeed both PbF_2 and $PbWO_4$-UF were tested.
Regarding the *ii*) some very interesting effects were observed that is why two different orientations of the prototype were studied. The first one was the "front" mode, where the injected electron finds upstream the crystal followed by the photo-sensors. The second one was the "back" mode, here Proto-0 was rotated by 180° degrees, meaning that SiPMs collect only light that has been uniformly reflected inside the crystal, avoiding effects linked to the Cherenkov light directionality. Clear effects of directionality were indeed showed in the "front" runs, especially in the charge sharing variable and time difference as a function of the beam position resulting in two population in the channels time difference distribution as observed in Figure 4-a. This effect is instead negligible in the "back" configuration (Figure 4-b), showing that this is a Cherenkov light propagation systematics, as also confirmed via MC optical simulation [5]. For the "front" run it was possible to perform an event-by-event correction thanks to the almost liner dependence between the asymmetry variable, consisting in the ratio between the two readout channels charge difference and the charge sum. When the correction was applied it was possible to recover a single population time difference distribution, as showed in Figure 4-c.

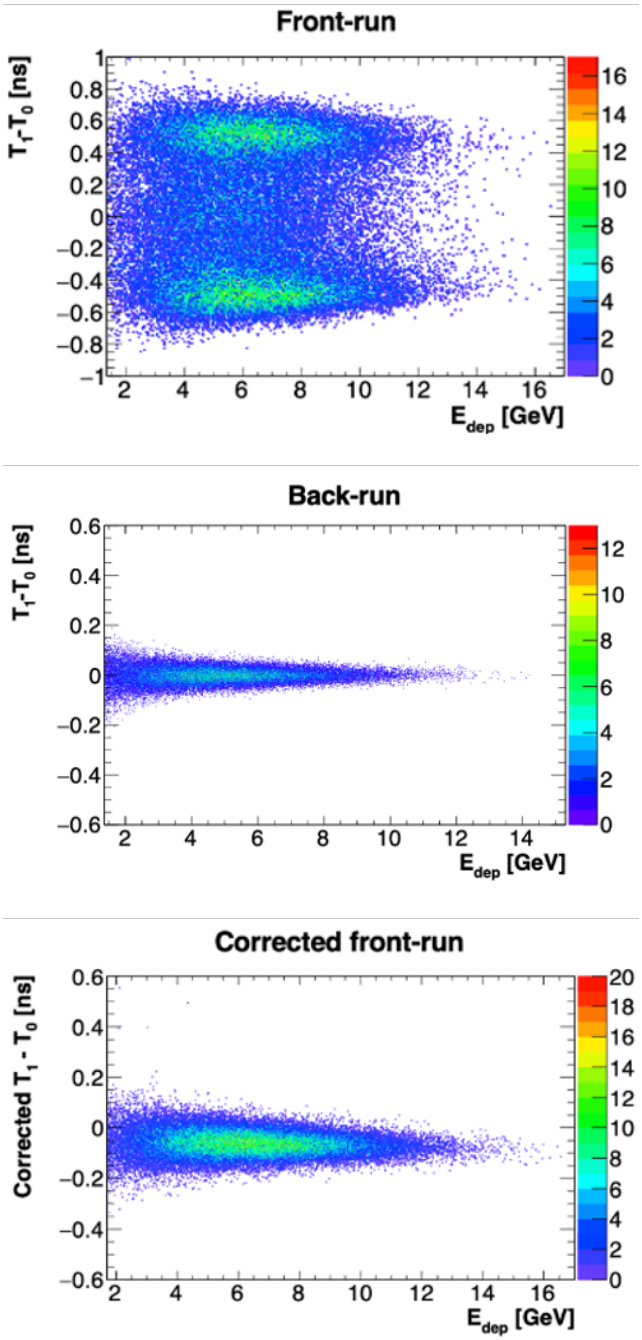

Fig. 4. a) Time difference between the two readout channels as a function of E_{dep}, for front configuration runs. The splitting of the distribution from position-dependent effects is evident. b) Distributions for runs in back configurations. c) Same distribution for front runs right after the event-by-event correction based on the dependence of the time difference from the charge asymmetry.

Starting from these distributions it was possible to estimate the time resolution from a Gaussian distribution fit applied on 10 E_{dep} slices. The results are presented in Figure 5 for all runs. It can be noted that the time resolution as a function of deposited energy was fitted using the function:

$$\sigma_{MT} = \frac{\sigma_{T1-T0}}{2} = \frac{a}{E_{dep}} \oplus b$$

where the subscript MT refers to the resolution obtained for the mean time for the two readout channels of the single calorimeter cell. Despite the higher light yield the timing performances of the front runs are still worse than the back runs, this is still due to some residual position-dependent light-transport effects. It should also be highlighted that, due to the purely Cherenkov nature of the light, the time resolution for PbF_2 is better than that for $PbWO_4$-UF in both configurations, even though the light yield for PbF_2 is only about half of that for $PbWO_4$-UF. Anyhow, the results for both crystals are deeply within the requirements set by the Muon Collider collaboration having indeed a worst-case time resolution for E_{dep} > 3 GeV less than 25 ps for PbF_2 and less than 45 ps for $PbWO_4$-UF.

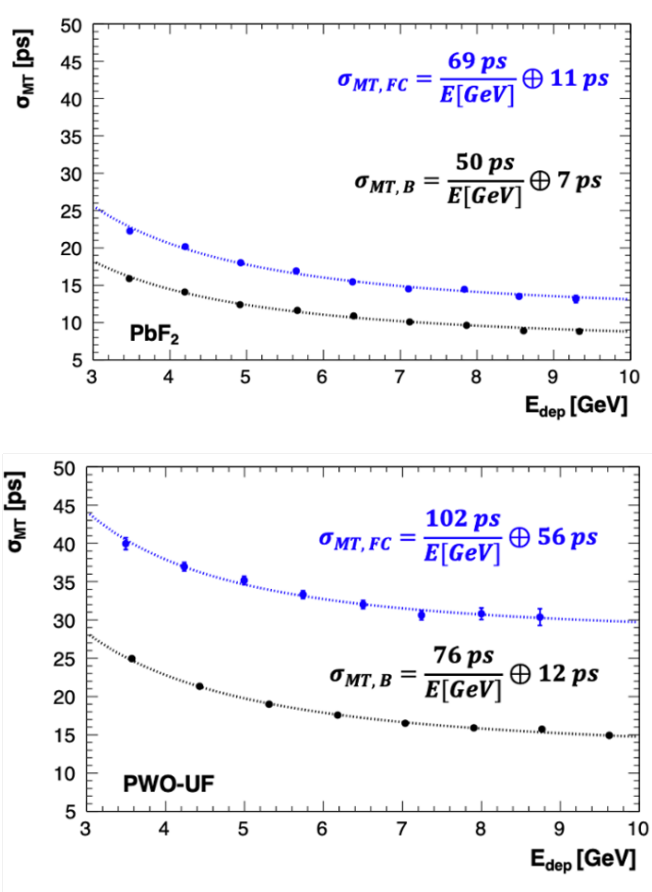

Fig. 5. Mean-time resolution of a single calorimeter cell for PbF_2 (a) and $PbWO_4$-UF (b) as a function of E_{dep} over the range 3-10 GeV. Front-configuration corrected runs ($\sigma_{MT,\ FC}$) are shown in blue, while back-configuration runs ($\sigma_{MT,\ B}$) are shown in black.

III. PROTO-1

The novel idea behind the Crilin ECAL is to use multiple layers of PbF_2 crystals and thin surface-mount device (SMD) SiPMs stacked on top to provide longitudinal information of the shower. In order to validate the design choices, a larger prototype was recently built, Proto-1. The Proto-1 design was optimized with the simulation studies starting from transverse and longitudinal dimensions of 0.7 R_M and 8.5 X_0 (~0.3λ) respectively. This size comes from a compromise of an acceptable containment of ~100 GeV electrons showers and cost constraints. Results will be extrapolated to the optimum length of the Muon Collider calorimeter of the order of 20 X_0.

Proto-1, in Figure 6, consist of two layers of 3×3 PbF_2 crystals, each readout by two series of two UV-extended SiPMs, as already done in Proto-0.

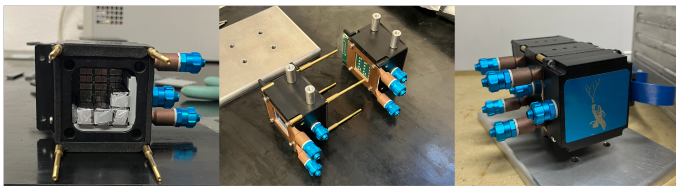

Fig. 6. Proto-1 images: a single module during crystal installation, the locking system and the prototype fully assembled.

Two stackable and interchangeable submodules assembled by bolting house the crystals, moreover the light-tight case also embeds the front-end electronic boards and cooling system. Indeed, the on-detector electronics and SiPMs must be cooled during operation, to improve and stabilize the performance of SiPMs against irradiation. This design can remove the heat load due to the increased photosensor leakage current after exposure to the expected 10^{14} n_{1MeV}/cm^2 fluence, along with the power dissipated by the amplification circuitry. The total heat load was estimated as 350 mW per channel. The Crilin cooling system consists of a cooling plant and a cold plate heat exchanger, made of copper, mounted directly over the electronic board. A glycol-based water solution passes through the deep drilled channels and absorbs the heat generated by the SiPMs. It will provide the optimum operating temperature for the electronics and SiPMs at 0/-10 °C.

The protype Front End Electronics (FEE), regulating a single module, is divided in two main parts (Figure 7): a SiPM board and the Mezzanine board. Each SiPM board, Figure 7-a, embeds 36 photo-sensors so that each crystal in the matrix has two separate and independent readout channels, consisting in a series of two 10 µm pixel-size SMD S14160-3010PS SiPMs [8]. These were chosen for their high-speed response, narrow signals and radiation hardness. Four SMD blue LEDs were also placed in between the SiPMs matrices in order to perform in-situ calibration, diagnostic and monitoring. The SiPMs are then connected via 50 Ω micro-coaxial transmission lines to a microprocessor-controlled Mezzanine Board. The Mezzanine Board oversees signal amplification and shaping, along with all slow control functions for all the 18 readout channels of the single layer. The SiPMs biasing is controlled by 12-bit DACs while regulated voltages, bias currents, and the temperature of the SiPM matrix are sensed via dedicated 12-bit ADC channels. The slow control routines are than handled by an onboard Cortex M4 microprocessor.

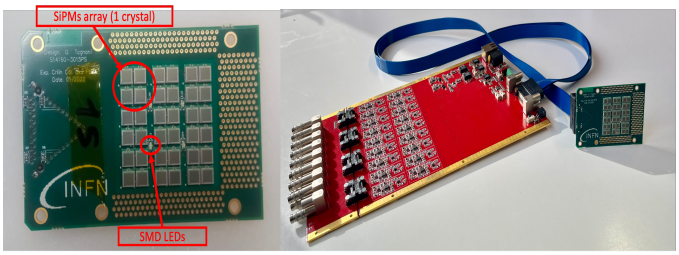

Fig. 7. FEE parts: the SiPMs board embedding the 36 photosensors and the Mezzanine board that bias, regulate and readout them.

Proto-1 performances will be evaluated in two dedicated Test Beam: the first one with 500 MeV electrons at BTF-LNF, whose analysis will be completed shortly, the second one at CERN-SPS H2 beamline with 120 GeV electrons. Time resolutions and a first estimation of the energy resolutions and the clusterization capability are going to be main interest of these tests.

IV. Conclusions

The Crilin calorimeter represents an innovative and promising choice for future collider experiments. It is a good compromise between homogeneous and sampling calorimeter and is well quoted as alternative solution to W-Si ECAL for future Muon Colliders. Several R&D steps were already made starting from radiation hardness campaigns on the single components and a Beam Test on a single layer prototype that showed very interesting results in terms time resolution. A bigger prototype, Proto-1, composed of two layers of 3×3 crystal matrices was recently developed and assembled. The characterization of this last prototype has already started with a Beam Test at BTF-LNF with 500 MeV electrons, for which the analysis is still ongoing. A second test beam will be also carried out at CERN-SPS H2 beamline with 120 GeV electrons. During these test beams it will be evaluated again the time resolution, given a first estimation of the energy resolution and tested the clusterization capability.
Once the performances of Proto-1 will be stated other irradiation campaigns will be performed with the aim of reaching the expected radiation level of the Muon Collider.
A huge R&D step will happen also during 2023 where a consistently bigger prototype, that will cover 1 Molier Radius, 20 radiation lengths and 1 interaction length, will be designed and built.

Acknowledgment

This project has received funding from the European Union's Horizon 2020 Research and Innovation program under the AIDAinnova project, grant no. 101004761, as well as from INFN projects RD_MUCOL.

References

[1] C. Accettura et al., "Towards a Muon Collider" (2023), https://arxiv.org/pdf/2303.08533.pdf
[2] N.Bartosik et al.,Simulated Detector Performance at the Muon Collider, (2022) https://arxiv.org/pdf/2203.07964.pdf
[3] Ceravolo S, et al., Crilin: A CRystal calorImeter with Longitudinal InformatioN for a future Muon Collider. JINST 17 (2022) P09033. doi:10.1088/1748-0221/17/09/P09033.
[4] A. Ferrari et al., "FLUKA: a multi-particle transport code", CERN-2005-10 (2005), INFN/TC_05/11, SLAC-R-773.
[5] Korzhik M, et al. Ultrafast PWO scintillator for future high energy physics instrumentation. Nucl. Instrum. Meth. A 1034 (2022) 166781. doi:10.1016/j.nima.2022.166781.
[6] Cemmi, A., et al. Radiation study of Lead Fluoride crystals. Journal of Instrumentation 17.05 (2022): T05015.
[7] Cantone C et al. Beam test, simulation, and performance evaluation of PbF2 and PWO-UF crystals with SiPM readout for a semi-homogeneous calorimeter prototype with longitudinal segmentation. Frontiers in Physics 11 (2023). doi:10.3389/fphy.2023.1223183.
[8] Hamamatsu S14160-3010PS datasheet, https://www.hamamatsu.com/content/ dam/hamamatsu-photonics/sites/documents/99_SALES_LIBRARY/ssd/ s14160-1310ps_etc_kapd1070e.pdf